한국기계가공학회지, 제16권, 제4호, pp.104～112(2017.08) ISSN 1598-6721(Print)
Journal of the Korean Society of Manufacturing Process Engineers,Vol.16, No.4, pp.104~112(2017.08) ISSN2288-0771(Online)

https://doi.org/10.14775/ksmpe.2017.16.4.104

Sand Casting Process Design for the Bush Parts of the Continuous Hot Zinc Plating Roll Applied to Wear-Resistant Alloy Cast Steel

Dong-Hwan Park*, Jae-Jung Yun*, Jin-Tae Hong**, Hyuk-Hong Kwon***,#

*Gyeongbuk Hybrid Technology Institute, **Bugang Special Co., Ltd,
***Depart. of Computer Aided Mechanical Engineering, Daejin Univ.

내마모 합금주강 소재를 적용한 연속용융아연도금설비 Roll용 부쉬의 사형 주조공정 설계

박동환*, 윤재정*, 홍진태**, 권혁홍***,#

*경북하이브리드부품연구원, **(주)부강특수산업, ***대진대학교 컴퓨터응용기계공학과

(Received 9 July 2017; received in revised form 16 July 2017; accepted 22 July 2017)

ABSTRACT

In the sand casting process, the flow of liquid metal affects the quality of casting products and their die life. To determine the optimal bush part design process, this study performed various analyses using commercial finite element analysis S/W. The simulation focused on the molten metal behaviors during the mold filling and solidification stages of sand casting. This study aims to develop methods to reduce the cost and increase the tool life of the continuous hot zinc plating roll.

Key words : Sand Casting(사형주조), Bush Parts(부시 부품), Stellite(스텔라이트), Wear-Resistant Alloy(마멸 저항 합금), Continuous Hot Zinc Plating Roll(주조 열간 아연 도금롤)

1. Introduction

There is a stainless steel as a corrosion resistant alloy casting material, and Cermet and Stellite alloy are representative wear-resistant casting alloys. Stainless steel has excellent corrosion resistance against nitric acid and sulfuric acid etc. at room temperature as compared with spheroidal graphite cast iron[1~5]. Cermet is a heat resistance material composed of metal and ceramic. It possesses heat resistance that makes it withstands high temperature and has oxidation resistance from corrosion, chemical resistance capable of withstanding chemicals, wear-resistance, high strength approaching to metal, and plasticity for easy processing, but it is brittle against impact[6]. Stellite alloy has excellent mechanical wear resistance and corrosion resistance at high temperature. Besides, it prevents corrosion, erosion, and wear and tear since chrome (Cr), carbon

Corresponding Author : hhkwon@daejin.ac.kr
Tel: +82-31-539-1972, Fax: +82-31-539-1970

(C), tungsten (W), and molybdenum (Mo) are added in cobalt. Further, because Stellite alloy has excellent antioxidant property due to its high temperature characteristics, and can be finished to excellent surface roughness. Stellite alloy has a low friction coefficient, thereby possessing excellent wear resistance. That is, it has excellent wear resistance and low friction coefficient, thus it is not damaged much when contacted with other metals, and has a very excellent property against erosion. In addition, it maintains high degree of hardness even at high temperature, making it be used in the belt parts or plungers in the pumps that require wear resistance and corrosion resistance.

Pouring temperature for the aluminum and magnesium die casting is at around 700℃, while the pouring temperature for the wear-resistant casting alloy Stellite is quite high at around 1,500℃[7~13]. Because the pouring temperature is high in the wear-resistant alloy cast iron material as compared with aluminum and magnesium alloys, precaution is required during handling. Zinc plating is a surface treatment technique for the steel products, which is implemented to extend life of steel and to improve its properties. The steel product produced by zinc plating is applied in many fields such as automobiles, appliances, and construction. Continuous hot-dip galvanizing devises an equipment with an objective of continuous production of galvanized steel sheet. Steel companies produce galvanized steel sheets using a hot-dip galvanizing method. Equipments involved in the continuous hot-dip galvanizing are zinc plating bath and chemical hot treatment. Among these, zinc plating bath is composed of sink roll, stab roll, and correct roll.

Galvanized steel sheet is produced by dipping a steel plate inside the zinc plating bath at around 500℃, making steel sheets pass through sink roll, stab roll, and correct roll. While going through this series of process, zinc is coated on the steel sheet during a specific duration. In the zinc plating bath, sink roll, stab roll, and correct roll are immersed and rotated, and sink roll is contacted with the general steel plate first after steel plate is immersed into the zinc plating bath, resulting it receives the largest load. Due to this, sink roll and bearings at both end of the sink roll are also simultaneously rotated, imposing serious abrasion in the bearing parts, consequently bearings are frequently replaced. Bearing parts at the sink roll is composed of bush and sleeve, and if bush and sleeve parts are frequently replaced due to wear during zinc plating, issues of low productivity, quality impairment, and working environment would be posed.

Bush for sink roll is a parts that is rotated in the continuous hot-dip galvanizing bath at around 500℃, therefore it is subjected to severe corrosion and wear-tear, spending a long-time to replace parts. To improve this problem, bush parts development is needed by implementing wear-resistant alloy casting materials and by designing a sand casting process [14~16]. This study aims to develop bush parts having a long life for sink roll in the continuous hot-dip galvanizing equipment by implementing a sand casting process for the wear-resistant alloy casting material capable of reducing production cost and extending die life.

2. Experimental Method

2.1 Wear test

For the wear test, pin-on-disk method is generally and widely being used. Pin-on-disk wear test was performed to evaluate friction coefficient for the wear-resistant alloy casting material. Pin and disk specimens were prepared for the wear test. Wear between metals is known to be affected by roughness of contacted surfaces, temperature, contacted condition, hardness, vertical load, and lubrication. The equipment and specimens for wear test are presented in Fig. 1, and testing conditions

are tabulated in Table 1. Wear test was performed with wear resistant alloy cast irons for pin as well as disk, with vertical load on the pin at 98N, while disk was not lubricated as shown in Fig. 2. Wear test results showed that the mean friction coefficients were in a range of 0.06~0.18 as in Table 2. The least coefficient 0.06 was obtained from T800 (pin) and Stellite 6 (disk) from the wear test.

Table 1 Conditions of wear test

Conditions		Value
Type		Pin-On-Disk
Material	Pin Disk	Stellite 6, Stellite 20, T800
Vertical load(N)		98
Sliding length(m)		1,695.6
RPM		100
Lubrication		None

Fig. 1 Wear testing machine

Fig. 2 Specimens for the wear test

Table 2 Mean friction coefficient results of the wear test

No.	Material		Mean friction coefficient
	Pin	Disk	
1	Stellite 6	Stellite 6	0.07
2	Stellite 6	Stellite 20	0.18
3	Stellite 6	T800	0.16
4	Stellite 20	Stellite 6	0.12
5	Stellite 20	Stellite 20	0.09
6	Stellite 20	T800	0.17
7	T800	Stellite 6	0.06
8	T800	Stellite 20	0.07
9	T800	T800	0.08

2.2 Design and fabrication of cast die

For sand casting process, wooden pattern was designed and prepared, and molding sand was made using this wooden pattern to make a mold, and then molten metal of desired material was poured. It has merits of sand casting process as compared with precision casting, and requires a low cost, enabling it to be implemented in the large casting or small-amounted products. The most important factor in the sand casting process is a modeling of the riser. Two riser models were set at the top of the product, height of the riser was set higher than 1/2 of the product's height, thickness was maintained as constant, and heating sleeve was attached.

A wooden pattern for bush was prepared, and was examined if it was matched with the drawing. Mold was made by mixing molding sand and sodium silicate at a specific ratio to prepare two sets each as shown in Fig. 3. Mold coating and alcohol at a specific ratio were mixed, the mixture was applied on the mold whose modeling was finished with a brush, so that joining would be done at the bottom. Raw material was loaded in the 100kg capacity electric furnace and was melted while checking temperature using an immersion type thermometer. Weight of the product unit was calculated and the most suitable ladle was arranged accordingly. The molten material was then poured into the mold with pouring temperature at 1,550℃. Before pouring the raw

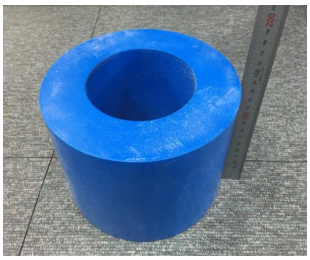

Fig. 3 Bush wooden pattern

material, deoxidant Ca-Si was applied on the top of the furnace. Besides, slacks were also regularly applied on the top of the furnace, so that non-metallic inclusion could be removed. Pouring speed for the raw material was set within five seconds. After pouring the raw material, exothermic agent was applied on the top of the mold, so that product could be solidified first. As a post-process, cleaning was performed caring not to damage the product while mold is dismantled. Cleaned product was then sent to the shot-blasting to make the surface free of impurities while inspecting by eyes. The sprue was cut caring not to damage the product. The roughing and finishing were followed according to the drawing. Finally, composition inspection, penetrant inspection, and dimensional inspection were performed.

3. Analysis of Casting Solidification

3.1 Analysis conditions

In order to analyze solidification of sand casting for the bush parts, casting product, core, sprue, runner, and riser were modeled with 3D, spitted into triangular meshes with gap between mesh at 10mm for sand casting mold, and at 5mm for casting product, core, and runner. Further, gravity direction setup, casting material, core material, sand casting material, heat transfer coefficient, pouring time, pouring temperature, cooling condition, and atmospheric temperature were input for the analysis. Fig. 4 shows bush parts, while Fig. 5 shows 3D modeling for the sand casting. The analysis conditions used in the casting solidification analysis are as in Table 3. The materials used for wear-resistant alloy steel were Stellite 6, Stellite 20, and T800, while silica(SiO_2) was used as a material for silica sand. Table 4 shows analysis conditions of sand casting mold for the bush parts.

The pouring temperature of molten metal was set at 1,550℃, and the pre-heating temperature of sand casting mold was set at 30℃. Fig. 6 shows finite element analysis model for the bush sand casting. Sand casting solidification analysis was performed using commercial software ProCAST. Fig. 7 shows solid fraction by alloys for Stellite 6, Stellite 20, and T800, as well as changing trends of solid according to the temperatures. In case of alloy T800, since temperature of the liquid phase was the highest, and mushy zone was narrow, it was expected that solidification would started at high temperature and processed quickly. Fig. 8 shows thermal conductivities by alloys, which confirmed that there is no large difference in the thermal conductivity according to the type of alloy.

Table 3 Simulation conditions of sand casting

Material	Stellite 6	Stellite 20	T800
Pouring time(sec.)	3~5	3~5	3~5
Pouring temp.(℃)	1,550	1,550	1,550
Mold temp.(℃)	30	30	30
Mold material	SiO_2	SiO_2	SiO_2
Heating sleeve	used	used	used

Table 4 Simulation conditions of sand casting mold

Division	Core	Mold
Material	Core blowing sand	Silica sand
Thermal conductivity (W/mk)	1	0.64~0.7
Density(kg/m3)	1,400	1,520
Specific heat (kJ/kg·K)	1	0.68~1.23
Initial temperature(℃)	30	30

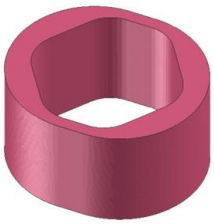

Fig. 4 Bush product

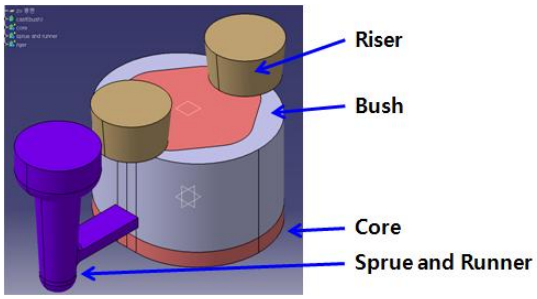

Fig. 5 3D Modeling of sand casting

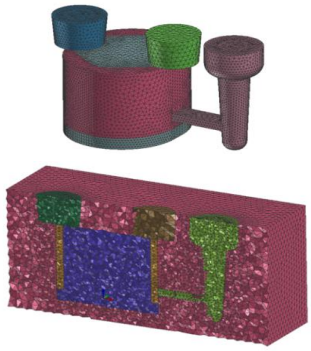

Fig. 6 FEM model of sand casting

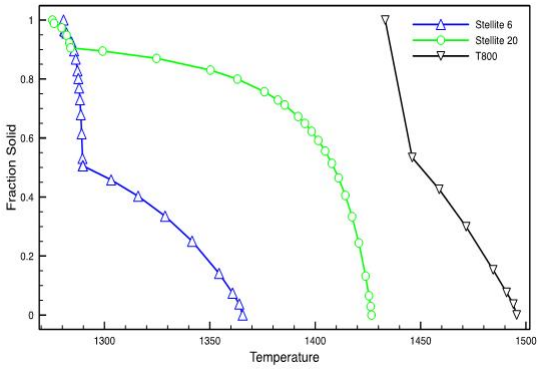

Fig. 7 Temperature-fraction solid curve

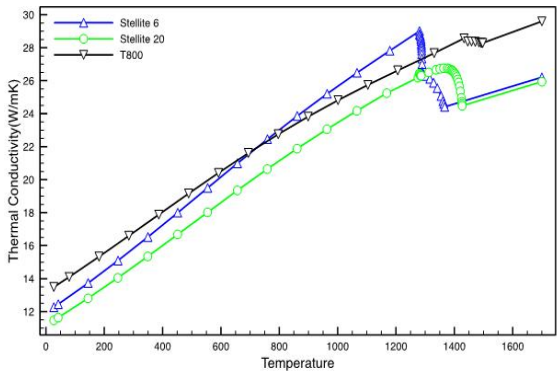

Fig. 8 Temperature-thermal conductivity curve

3.2 Analysis results

For the temperature distribution by alloy according to filling rate, temperature zone for liquid line of the alloy pouring temperature at 1,550℃ could be confirmed by solid fraction by alloy as shown in Fig. 8. T800 at the highest zone in the liquid line was cooled first, and the cooling speed was in the order of T800, Stellite 20, and Stellite 6 as shown in Fig. 9. Pouring time for T800 became elongated since it was cooled faster than Stellite 6 and Stellite 20, thus liquidity became slower as shown in Fig. 10. Fig. 11 shows the casting analysis results that performed to predict casting behavior showed Mis-run(casting defect). Since possible Mis-run portion for alloy T800 were found in orange- and red-colored products, Mis-run could be prevented by increasing pouring temperature.

Fig. 12 shows the freezing point analysis results for the sand casting. Freezing points were appearing inside the parts in all the alloys due to insufficient feeding of molten metal by the riser. Fig. 13 shows analysis results for shrinkage cavities in the sand casting. A large shrinkage was expected at the center of Y axis in the bush, and the shrinkages were on an around 4.5cc for Stellite 6, 10.3cc for Stellite 20, and 16.7cc for T800. In T800, shrinkage cavity was brittle, thus position of riser needed to be changed. Therefore, position of the riser for

T800 bush was shifted to the side where breadth of the product was wider. The result was that shrinkage cavity from inside of the product was removed as shown in Fig. 14, but the shrinkage cavity was appeared at the connected portion between the riser and the product, which implies that the shrinkage cavity would appear on the surface after riser is removed. Secondary solidification analysis was carried out after changing riser position and increasing height by 20mm for the bush parts. Shrinkage cavity was not found at the connected portion to the riser as shown in Fig. 15.

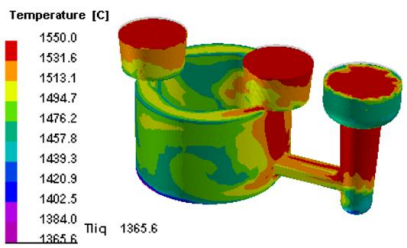

(a) Stellite 6

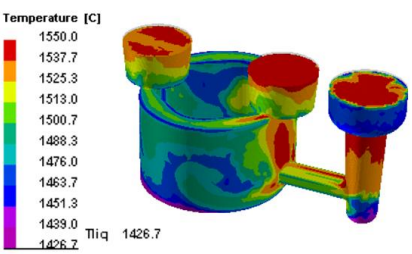

(b) Stellite 20

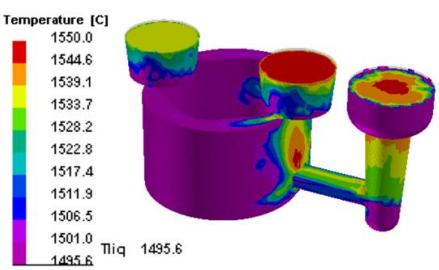

(c) T800

Fig. 9 Temperature distribution with the filling rate of 98%

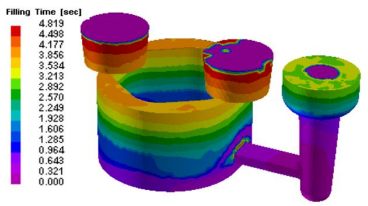

(a) Stellite 6

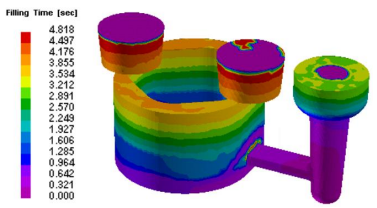

(b) Stellite 20

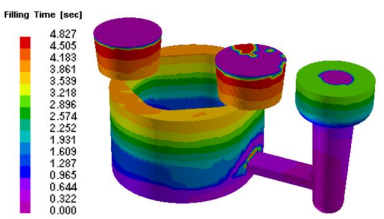

(c) T800

Fig. 10 Filling time of sand casting

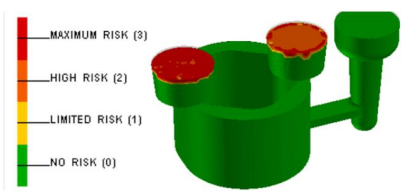

(a) Stellite 6

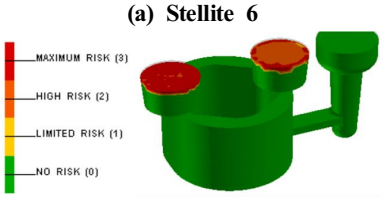

(b) Stellite 20

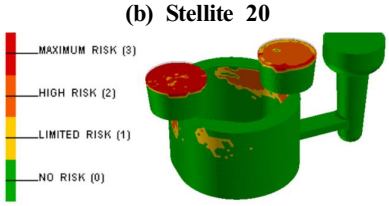

(c) T800

Fig. 11 Mis-run of sand casting

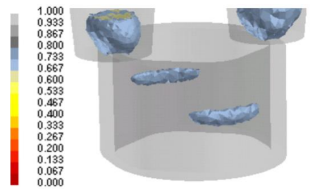

(a) Stellite 6

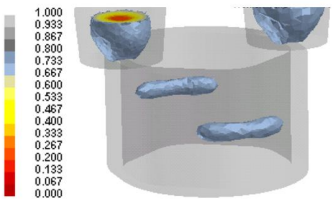

(b) Stellite 20

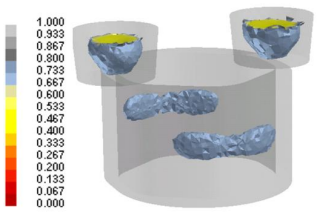

(c) T800

Fig. 12 Freezing point of sand casting

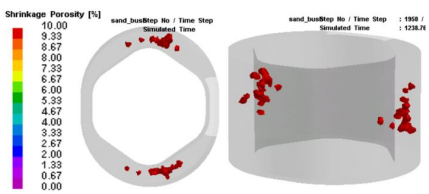

(a) Stellite 6

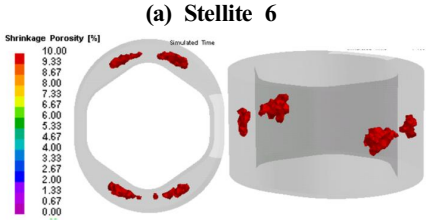

(b) Stellite 20

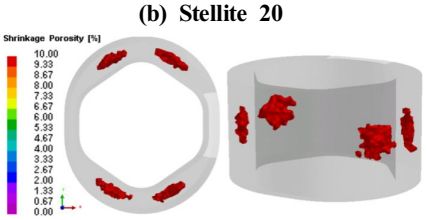

(c) T800

Fig. 13 Shrinkage cavity of sand casting

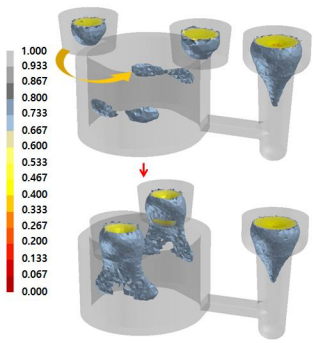

Fig. 14 Freezing point of 1st modified bush of T800

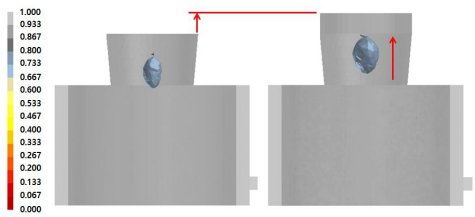

Fig. 15 Freezing point of 2nd modified bush of T800

4. Test Results and Discussion

Fig. 16 shows the casting mold after completion of the modelling. Modelling was carried out with a specific mixing ratio between molding sand and sodium silicate, while shaping agent and alcohol were mixed at a specific ratio, stirred, and then applied on the completed casting by brush. Casting solidification analysis result for the Stellite 6, Stellite 20, and T800 under the pouring temperature at 1,550℃ showed that high possibility of Mis-run was in the alloy T800, whereas Mis-run was not found from the Stellite 6 and Stellite 20. The high possibility of Mis-run in the T800 is attributable by high liquid temperature and the structural restriction as it has the narrowest solidification in the microscopic area. Further, though it was judged that casting should be done at higher temperature than the suggested pouring temperature(1,550℃), another defects were concerned at this temperature. Therefore, pouring temperature was decided as 1,55 0℃.

Shrinkages were expected inside products for all the three alloys due to riser that was located at the Y axis of the product. Especially in the T800, the largest amount of shrinkage was found from T800. Therefore, riser location was changed towards the Y axis and the riser height was increased by 20mm during fabrication of the casting so that good bush product without shrinkage cavity inside of it could be secured. Fig. 17 shows the pouring process into the sand casting, while Fig. 18 shows the bush parts executed by the sand casting. Fig. 19 shows the bush product made of wear-resistant alloy casting, while Fig. 20 shows the bush assembly executed by the sand casting. The bush casting parts made of wear-resistant alloy casting was then processed with roughing and finishing, and finally composition inspection, penetrant inspection, and dimensional inspection were conducted for the finished products.

Fig. 16 Sand casting mold

Fig. 17 Pouring process of sand casting

Fig. 18 Bush of sand casting

Fig. 19 Final bush product of sand casting

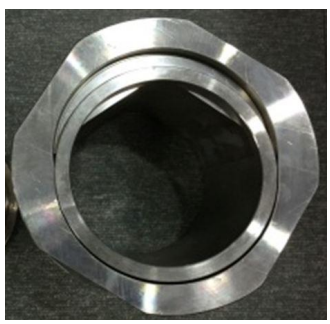

Fig. 20 Final bush assembly product of sand casting

5. Conclusions

Sand casting process was suggested in this study in order to develop bush parts for continuous hot-dip galvanizing roll with wear-resistant alloy casting material. Wear test, casting solidification analysis, designing and fabrication of the mockup mold, and performance evaluation for the trial products were conducted in order to design a sand casting process for the bush parts. The findings are as follows;

1. The mean friction coefficient was determined through friction test in order to execute bush parts having a long life. The lowest mean friction coefficient was found from the T800 and Stellite 6, therefore these were selected as materials for the bush parts.
2. Bush parts was designed into the sand casting, casting solidification analysis was performed according to wear-resistant alloy casting, and then temperature distribution, pouring time, Mis-run, and shrinkage cavity according to the filling rate were investigated for the optimum

casting methods.

3. Casting solidification analysis revealed that position of the riser was an important factor during bush parts designing with a sand casting, and the position of the riser could be validated with the analysis and the trial products.

References

1. Ann, S. J., Kang, M. R., Seo, D. S., Kim, Y. H., Lee, K. H., Kim, H. S., "A Study on the High Temperature Strength of Ferritic Stainless Cast Steels," Journal of Korea Foundry Society, Vol. 18, No. 6, pp. 563-569, 1998.
2. Lee, K. D., Ha, T. K., Jung, J. Y., "Characterization of High Temperature Mechanical Properties of Cast Stainless Steels for Exhaust Manifold," Transactions of Materials Processing, Vol. 18, No. 3, pp. 217-222, 2009.
3. Kim, S. W., Park, J. S., Khalil, K. A., "Effects of C, Si and RE on Microstructures of DCI using Permanent Mold Casting," Journal of Korea Foundry Society, Vol. 26, No. 4, pp. 174-179, 2006.
4. Kim, S. T., Park, Y. S., "Effects of Copper and Sulfur Additions on Machinability Behavior of High Performance Austenitic Stainless Steel," Metals and Materials International, Vol. 15, No. 2, pp. 221-230, 2009.
5. Kayali, Y., Buyuksagis, A., Yalcin, Y., "Corrosion and Wear Behavior of Boronized AISI316L Stainless Steel," Metals and Materials International, Vol. 19, No. 5, pp. 1053-1061, 2013.
6. Kim, Y. S., Kwon, W. T., Seo, M. S., Kang, S. H., "Tool Performance of New Wear-Resistant Cermets," International Journal of Precision Engineering and Manufacturing, Vol. 13, No. 6, pp. 941-946, 2012.
7. Yoon, H. S., Oh, Y. K., "Numerical Study on Thermal Deformation of AC4C and AC7A Casting Material," Journal of The Korean Society of Manufacturing Technology Engineers, Vol. 20, No. 5, pp. 541-546, 2011.
8. Kim, E. S., "Die Casting Process Design for Gear Housing of Automobile Transmission by using MAGMA Soft," Transactions of Materials Processing, Vol. 14, No. 2, pp. 112-120, 2005.
9. Kim, Y. C., Cho, S. W., Cho, J. I., Jeong, C. Y., Kang, C. S., "Optimization of the Thin-walled Aluminum Die Casting Die Design by Solidification Simulation," Journal of Korea Foundry Society, Vol. 28, No. 4, pp. 190-194, 2008.
10. Han, J. J., Kwon, H. W., "Effects of Alloying Element and Grain Refinement on the Tensile Properties of Mg-Alloy Casted with Sand Mold," Journal of Korea Foundry Society, Vol. 31, No. 4, pp. 212-217, 2011.
11. Choi, S. R., Kim, C. K., Park, K., Oh, C. H., "Development of Precision Casting Technology for Lnlet Gear Box using Selective Laser Sintering," Journal of the Korean Society of Machine Tool Engineers, Vol. 9, No. 1, pp. 30-37, 2000.
12. Han, K. T., "Research on the Mold Design of Motor Housing using Die Casting Process," Journal of the Korean Society of Manufacturing Process Engineers, Vol. 14, No. 5, pp. 36-41, 2015.
13. Kim, J. D., Yoon, M. C., "Decision-Making of Casting Process using Expert System," Journal of the Korean Society of Manufacturing Process Engineers, Vol. 13, No. 6, pp. 54-60, 2014.
14. Nawi, I., Siswanto, W. A., Ismail, A. E., "A Study of Auto Pour in Sand Casting Process," Applied Mechanics and Materials, Vol. 660, pp. 74-78, 2014.
15. Kim, M. G., Kim, Y. J., "Investigation of Interface Reaction between TiAl Alloys and Mold Materials," Metals and Materials International, Vol. 8, No. 3, pp. 289-293, 2002.
16. Kang, D. M., Park, K. D., Park, J. H., "High Temperature Creep Strength of Mg-Nd-Zr-Zn Alloy in Sand Castings," Journal of the Korean Society of Manufacturing Process Engineers, Vol. 10, No. 6, pp. 83-88, 2011.